# Electronic Control over Attachment and Self-Assembly of Alkyne Groups on Gold

**Qing Li,[†,⊥] Chengbo Han,[‡,⊥] Miguel Fuentes-Cabrera,[†,§,*] Humberto Terrones,[†] Bobby G. Sumpter,[†,§] Wenchang Lu,[‡,§] Jerry Bernholc,[‡,§] Jieyu Yi,[†] Zheng Gai,[†] Arthur P. Baddorf,[†] Petro Maksymovych,[†,*] and Minghu Pan[†,*]**

[†]Center for Nanophase Materials Sciences, Oak Ridge National Laboratory, Oak Ridge, Tennessee 37831, United States, [‡]Center for High Performance Simulation and Department of Physics, North Carolina State University, Raleigh, North Carolina 27695, United States, and [§]Computer Science and Mathematics Division, Oak Ridge National Laboratory, Oak Ridge, Tennessee 37831, United States. [⊥]These authors contributed equally to this work.

**ABSTRACT**

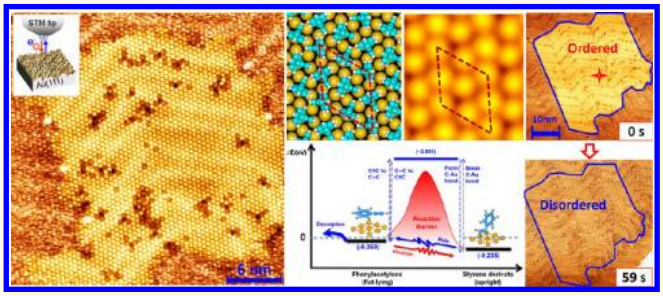


**Self-assembled monolayers are the basis for molecular nanodevices, flexible surface functionalization, and dip-pen nanolithography. Yet self-assembled monolayers are typically created by a rather inefficient process involving thermally driven attachment reactions of precursor molecules to a metal surface, followed by a slow and defect-prone molecular reorganization. Here we demonstrate a nonthermal, electron-induced approach to the self-assembly of phenylacetylene molecules on gold that allows for a previously unachievable attachment of the molecules to the surface through the alkyne group. While thermal excitation can only desorb the parent molecule due to prohibitively high activation barriers for attachment reactions, localized injection of hot electrons or holes not only overcomes this barrier but also enables an unprecedented control over the size and shape of the self-assembly, defect structures, and the reverse process of molecular disassembly from a single molecule to a mesoscopic length scale. Electron-induced excitation may therefore enable new and highly controlled approaches to molecular self-assembly on a surface.**

**KEYWORDS:** scanning tunneling microscopy · molecular reaction · self-assembly · 3D tethering

Alkanethiol self-assembly on gold has produced numerous new applications involving surface functionalization, paved ways to new research areas, such as molecular electronics,[1,2] and enabled dip-pen nanolithography.[3] Much of the success of this particular system is rooted in the 3D character of the alkanethiol self-assembled monolayers (SAMs), where the molecular tails are decoupled from the metal support, thereby forming dense packing and enabling a subsequent attachment of complex functional molecules to surfaces.[4,5] Besides that, thiol self-assembly can be prepared and can maintain its structure in air condition. However, thiol self-assembly also has some disadvantages, involving the numerous defects within the monolayer.[5−9] Furthermore, on a fundamental level, relying on thermal fluctuations to drive the surface attachment reactions reduces the degree of control over the interfacial chemistry and necessitates nontrivial approaches[10,11] to nanoscale patterning or substitution reactions within the self-assembled layer.

A key challenge is that a large number of potentially interesting molecules do not possess a thermally activated pathway to self-assembly, particularly for the formation of the all-important three-dimensional monolayer. Indeed, despite the fact that almost every molecule studied on the gold surface exhibits some forms of 2D assemblies, very few molecules so far have yielded 3D assemblies that would rival thiol-derived monolayers. An intriguing alternative anchor is the alkyne group.[12−16] On the basis of early theoretical analysis,[12] the alkyne group can form several stable bonding derivatives on the prototypical Au(111) surface. Furthermore, some of the derivatives can maintain $\pi$-conjugation down to the gold surface,[16] which may be beneficial for electron transport across metal−organic interfaces. However, theoretical calculations suggested that the stability of the alkyne bond itself gives rise to a very high activation barrier for the attachment reaction and largely precludes

* Address correspondence to panm@ornl.gov, fuentescabma@ornl.gov, maksymovychp@ornl.gov.

Received for review August 16, 2012 and accepted September 26, 2012.

**Published online** 10.1021/nn303734r

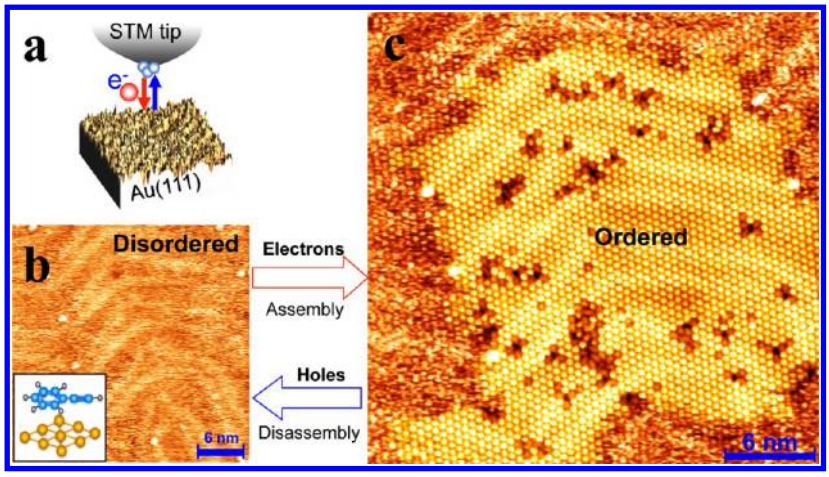


**Figure 1. Transition between the disordered phase and the ordered phase by the tip-induced reaction on the Au(111) surface. (a) Schematic drawing shows the experimental setup of the tip-induced reactions. (b) Topographic STM image of the disordered phase. Inset is the schematic drawing of a flat-lying physisorbed phenylacetylene molecule. (c) Topographic STM image of ordered structure at the same location as (b) after the reaction.**

a thermally activated reaction pathway.[12] To make SAMs with alkyne groups, experiments have therefore focused on the oxidation of the alkyne group,[16,17] but a clear ordered arrangement has so far been elusive and the requirement for an oxidant significantly complicates the methodology for the self-assembly and the chemistry involved. Whether or not alkynes will ever compete, substitute, or just become complementary to alkanethiols is an open question because, so far, direct chemical attachment (without extra reagents) has not been possible.

Here we demonstrate that electron-induced reactions (Figure 1a) of the alkyne group on the gold surface overcome the challenge of the prohibitively high activation barrier and produce a well-ordered self-assembled structure composed of upright molecules with covalent bonding to the surface (Figure 1c). Moreover, the electron-induced reactions can be finely tuned through the choice of the excitation conditions and localized down to a single-molecule scale, altogether allowing for an unprecedented control over the assembly process. Our presented electronic control strategy thus enables fast, reversible, and inherently nanoscale control over the chemistry of the anchor bond in a broad family of new compounds including molecules where thermally activated self-assembly reactions are not available.

## RESULTS AND DISCUSSION

The building blocks of our experiments are the phenylacetylene molecule and the Au(111) surface. Imaging the Au(111) surface by scanning tunneling microscopy (STM) after deposition of phenylacetylene at 85 K yields a fuzzy image with a clearly persistent topography of the $22\times\sqrt{3}$ herringbone reconstruction (Figure 1b). The fuzziness indicates a mobile molecular overlayer,[18,19] which in our case is composed of physisorbed flat-lying phenylacetylene molecules on gold[20] (also see Supporting Information, Figure S1). The fuzzy STM image is dramatically transformed if the surface area is scanned by an STM tip with positive sample bias. As seen in Figure 1c, a clear ordered structure emerges, with an approximately hexagonal packing of molecular features. The ordered island slowly "grows" accompanied with the tip scanning (see Supporting Information, Figure S2). Once established, the ordered structure remains stable for a long period of time (over 24 h), independent of tunneling conditions or even the presence of an STM tip. The stability of the image indicates a different and stronger bonding between phenylacetylene molecules and the gold surface. At the same time, the underlying herringbone reconstruction is not lifted, indicating that the Au surface is not significantly perturbed in the process, in stark contrast to the self-assembly of alkanethiols.[21,22] The area of the surface that undergoes this disorder−order transition can be hundreds of square nanometers, accommodating thousands of ordered molecules (see Supporting Information, Figure S2).

Building the ordered structure is dependent on the net injected charge, which can in turn be controlled by the scan rate of the STM tip. At the chosen sample bias of +1 V, the conversion is negligible at a scan rate exceeding 300 nm/s. By investigating the net assembly yield as a function of scan rate, we derived a linear plot with a slope of $6.1 \times 10^{-9}$ molecule/electron (Figure 2a). This value provides an estimate for a lower bound for the net reaction yield under the specific imaging conditions since we cannot resolve the density of molecules within the fuzzy image and it is likely lower that that within the self-assembled arrangement. We believe that the attachment reaction is primarily produced by rastering the tip across the surface because of the need for a high current density, which will compensate for a relatively low $10^{-9}$ yield of the

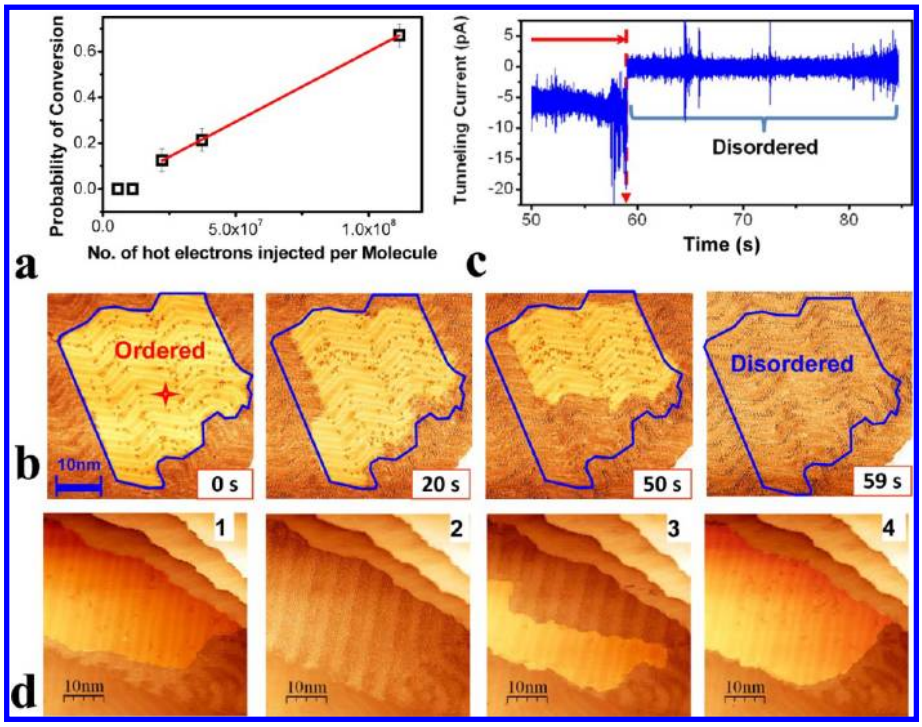


**Figure 2. Electron-induced controllable and reversible transition between the ordered and disordered phase. (a) Probability of conversion from the disordered to ordered configuration *vs* the average number of electrons injected per molecule. The tunneling junction was set with a sample bias of +1.6 V and tunneling current of 50 pA. (b) Snapshots of the disassembly process after 0, 20, 50, and 59 s of hole injection into the surface, using voltage pulses at −0.5 V sample bias (images acquired at $V_{bias}$ = +1 V, $I_{set}$ = 30 pA). A star in the image at 0 s indicates the location on the surface where the negative pulses were applied. (c) Time dependence of the tunneling current signal during the disassembly process, showing an abrupt drop of current when the ordered domain completely disappears. (d) Series of subsequent images showing the reproducibility and controllability of the phase transition. The ordered structures emerge by slow scanning with a positive bias voltage, and the self-assembled layer is destroyed by a negative bias pulse. The bias voltage during scanning (30 nm/s) is set at +1 V, and the tunneling current is 20 pA. The negative bias for the pulse is −0.6 V.**

reaction. Other tip effects cannot be ruled out at this point.

While the injection of hot electrons causes the molecules to react and self-assemble, hot holes (supplied by negative sample bias) cause a highly controllable disassembly (Figure 2b). In this case, the STM tip does not have to raster the image. Instead, hot holes are injected into the surface from a single position under the tip, and disassembly occurs in a large area surrounding the tip−surface junction, as seen in a series of images in Figure 2b. Disassembly is always initiated at the periphery of the ordered structure and proceeds inward to the center. Once the disassembling front reaches the tunnel junction, the tunneling current drops to zero (the plot of recorded tunneling current *vs* time in Figure 2c), indicating the conversion of the molecules under the tip. To investigate the reaction rate, we create ordered islands with different sizes at the same region, as shown in Figure 3b. We studied the disassembly process of these ordered structures using a fixed pulse voltage (−0.5 V). We found that the time needed to erase an island of a given area scales linearly with its size (Figure 3a). Thus the net electron fluence scales linearly with the number of molecules, identifying single-electron kinetics with $6.3 \times 10^{-7}$ molecule/electron, which is at least 2 orders of magnitude higher than that for the assembly reaction. It is also noteworthy that those islands are created and erased repeatedly in the same region, suggesting a good controllability and reversibility of the reaction.

The order−disorder transition is completely reversible in the same area of the surface, allowing one to create, erase, and recreate the ordered structures simply by varying the tunneling conditions and scan parameters, as shown in a series of consecutive STM images in Figure 2d. It is noteworthy that the density of molecules in the ordered structure is higher than that in the disordered phase. Actually, the nearest distance between adjacent flat-lying molecules is ~8 Å on the Au(111) surface.[20] In contrast, the nearest neighbor distance within the self-assembled layer in Figure 4a is about 6.15 Å. Extra molecules can be supplied either by the molecular diffusion on the gold surface or by deposition from the tip. The complete reversibility of the process strongly suggests that diffusion on gold is the dominant process. This level of control over the self-assembly/disassembly processes enabled by electron/hole-induced reactions is largely unprecedented.

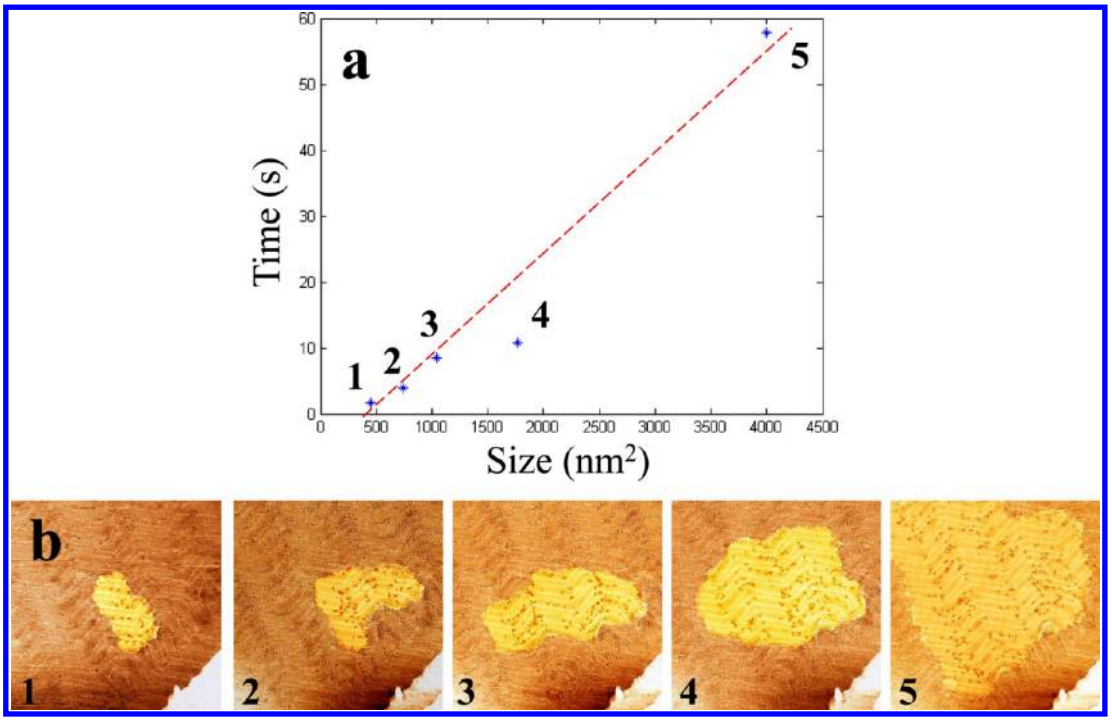


**Figure 3. Size dependence of the erasing process. (a) Plot showing the time needed to erase an ordered molecular island *vs* the island size. (b) Topographic images of the molecular islands to be disassembled. It is noteworthy that those islands are created and erased repeatedly in the same region, suggesting a good controllability and reversibility of the reaction. The bias pulse used to erase the order island is −0.5 V.**

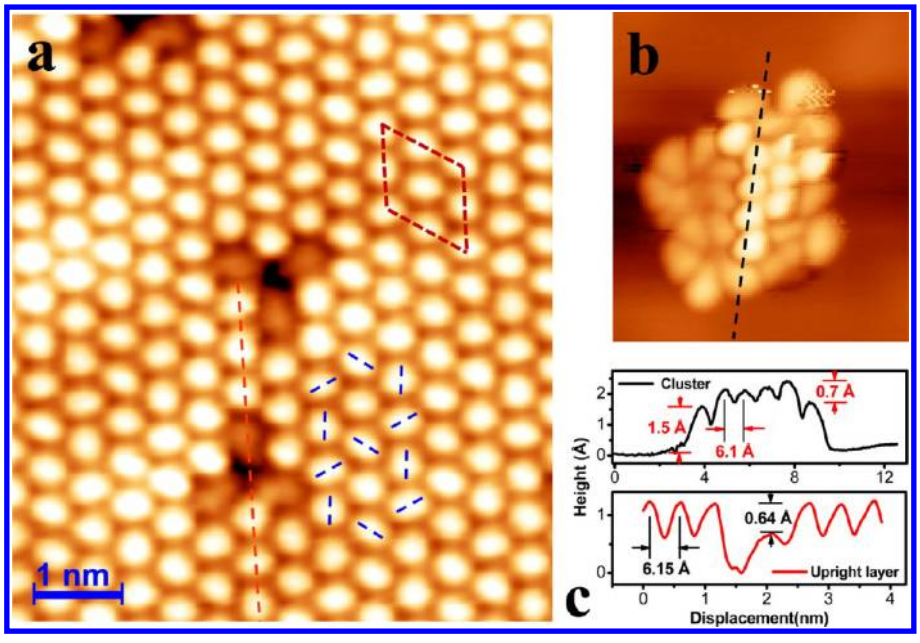


**Figure 4. Evidence of the flat-lying and upright orientation of the molecule in the disordered and ordered phases. (a) High-resolution STM image ($V_{bias}$ = +1.6 V, $I_{set}$ = 50 pA) of the ordered structure. The dashed lines indicate the pinwheel-like structure of ordered molecules, originated from the T-junction of the upright phenyl rings. Red rhombus shows the unit cell of the ordered structure. (b) Highly resolved STM image acquired at 28 K shows the coexistence of flat-lying and upright molecule species. The upright molecules form similar hexagonal packing in both size and orientation with the ordered phase shown in (a). The flat-lying molecules have a height of 1.5 Å and elongated shape, similar to the defect in (a). (c) Line profiles across the defect of (a) and along the island in (b).**

The reversibility of the self-assembly process (Figure 2d) strongly argues that the phenylacetylene molecule maintains its stoichiometry during the disorder−order transition. According to previous reports,[12] phenylacetylene molecules may assume both flat-lying and upright configurations on metal surfaces. However, the intermolecular interactions between flat-lying molecules could only be attractive for six nearest neighbor

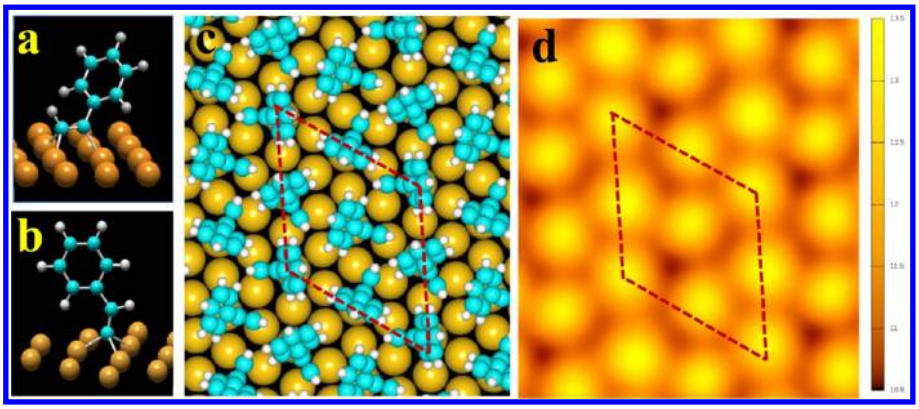


**Figure 5. Structural model of the self-assembled layer as well as the simulated image. (a) Relaxed model of a single styrene derivative on Au(111). (b) Relaxed model of a single phenylvinylidene on Au(111). (c) Top view of DFT-relaxed model for the self-assembled styrene derivative monolayer on the gold surface. (d) Simulated constant current image of the self-assembled styrene derivative monolayer.**

molecules with the intermolecular spacing of ~8 Å on the Au(111) surface.[20] In contrast, the self-assembled layer in Figure 4a is composed of hundreds of molecules, arranged with well-defined translational symmetry, and with a nearest neighbor distance of about 6.15 Å. Neither the continuous packing nor the packing density of the self-assembled layer are compatible with the flat-lying orientation. We therefore assign the building blocks to phenylacetylene derivatives with upright orientation of the phenyl ring.

The upright orientation of the molecule is directly supported by our low-temperature experiments carried out at 28 K, where the flat-lying molecules are stabilized. In Figure 4b, we observed two kinds of protrusions. The dark ones are flat-lying molecules, not only because their elongated shape is similar to that seen in previous observations,[20] but also because their apparent height (0.15 nm) corresponds to flat-lying phenyl rings.[20] The STM apparent height between the dark and bright protrusions is about 0.7 Å (Figure 4c), much smaller than the height of a flat phenyl ring, suggesting the upright configuration for the bright ones. Indeed, the STM apparent height difference between flat-lying and upright molecules on the Si(100) surface[23] is 0.8 Å, in good agreement with our observation at 28 K. Interestingly, the upright brighter molecules at 28 K are identical to the building blocks of the self-assembled phase at 85 K, with regard to the shape of molecular features and their similar hexagonal packing motif in both size (nearest neighbor molecular distance 6.1 Å) and orientation. Meanwhile, the flat-lying molecules, which are known to show an elongated shape and have a height of 1.5 Å, bear strong resemblance to the defects inside the self-assembled structure at 85 K, with also a 0.7 Å height difference compared with the upright molecules (Figure 4a,c). By the careful analysis of the STM images acquired at 28 and 85 K, we conclude that the self-assembly island after reaction at 85 K is composed of molecules with upright configurations. Finally, although a detailed analysis of the defects is outside the scope of the present discussion, the observed motion, emergence, and disappearance of the defects (see Supporting Information, Figure S3) clearly illustrate the transition between flat-lying and upright molecules on a single-molecular level.

Corroboration of the experimental results and elucidation of the underlying mechanisms were obtained from extensive density functional theory (DFT) studies that examined the binding energy of 20 different configurations, including both upright configurations on different surface sites and unreacted flat-lying phenylacetylene over a gold surface (see Supporting Information, Figure S4 and Table S1). Besides that, DFT results indicate that an unreacted, upright phenylacetylene is less stable than a flat-lying molecule, and in that upright configuration, it can only be bound weakly with the Au surface at ultralow temperature. Such weak physisorption would not be strong enough to attach an upright phenylacetylene molecule to form a robust self-assembly monolayer. Moreover, the unreacted upright phenylacetylene molecule extends much higher above the surface than the flat-lying one, which is incompatible with the 0.7 Å height difference observed by STM.

For the case of chemisorption, the reversibility of the reaction (Figure 2d) rules out deprotonation[12] of phenylacetylene in the process. Two candidate structures of the reacted alkyne group can satisfy this constraint, both similar to the structures proposed in ref 12. The first structure (hereafter, styrene derivative, Figure 5a) is produced by a partial dissociation of the triple bond and bonding with the C−C double bond approximately parallel to the surface. The second structure involves tautomerization of the ethyne group, with the proton moving to the C2 position to form a bonded phenylvinylidene (Figure 5b). The DFT calculations (see Supporting Information, Figure S4 and Table S1) yield the overall largest binding energy (−421 meV) for the phenylvinylidene, followed by the styrene

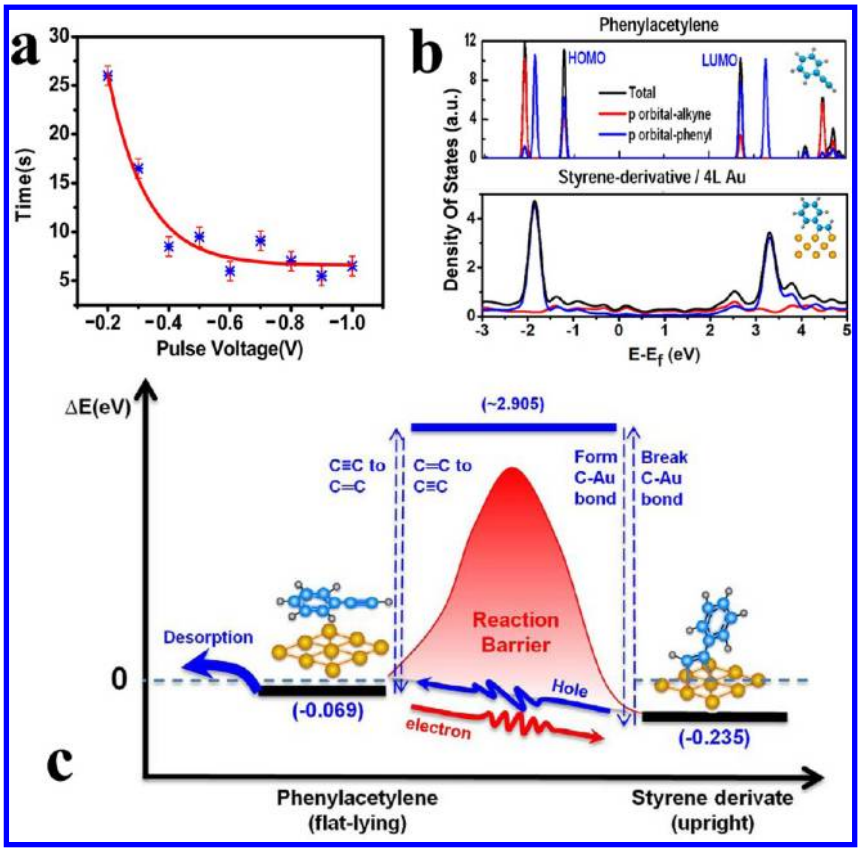


**Figure 6. (a) Pulse voltage dependence of the disassembly time at fixed gap distance ($V_{bias}$ = +1 V, $I_{set}$ = 30 pA). The error bars account for the scatter in the sizes of the ordered and disordered islands. This dependence can be phenomenologically fitted by exponential decay (red curve) with a threshold about −0.2 V. (b) Calculated projected density of states (PDOS) for two molecular configurations (top to bottom): gas-phase phenylacetylene, styrene derivative on four layers of Au. The corresponding structures are exhibited at the right corner of each plot. All PDOS plots are aligned according to deep filled states. (c) Schematic illustration of the relevant energies for nonthermal reaction pathways of assembly/disassembly processes. Δ*E* is the binding energy.**

derivative (−235 meV) and then the flat-lying phenylacetylene (−69 meV). In the most stable configuration of phenylvinylidene (Figure 5b), $\pi$-conjugation between the double bond and the phenyl ring is maintained and the molecule is oriented normal to the surface. In contrast, the styrene derivate on Au(111) is tilted and its phenyl ring is significantly twisted (Figure 5a), both as a result of strong Pauli repulsion between the ortho-proton of the phenyl ring and the gold atoms of the surface.

The styren -derivative is well-accepted as an upright structure for phenylacetylene adsorbed on Cu(100), Rh(100), and Cu(111) surfaces,[14,15,23] and it is more consistent than phenylvinylidene with a small height difference (0.7 Å) observed by STM. On the basis of these facts, we composed a structural model for the ordered phase by placing an upright styrene derivate in a compact arrangement within a layer, with the phenyl rings rotated by at least 60° relative to each other. The structure relaxed by DFT is shown in Figure 5c. The distance between the nearest neighbors is in the range from 5.09 to 6.74 Å, in good accord with the experimental value of 6.15 Å. Notably, the simulated constant current image (Figure 5d) matches the STM topographic image (Figure 4a) exceptionally well, clearly indicating a "pinwheel-like" structure, that implies "T-like" junctions between the molecules. The T-like junctions demonstrated in Figure 5c originate from the CH/$\pi$ hydrogen bonding between upright phenyl rings,[24] which on the other hand never happens between flat-lying ones. Such junctions are well-known for aromatic molecules, including phenylacetylene derivatives.[12] The energy gain of 0.5−2 kcal/mol per junction[24] explains the origin of the attractive interactions within the self-assembled layer.

The conversion of phenylacetylene to the styrene derivate on Au is borderline favorable energetically with the reaction enthalpy of only −156 meV (see Supporting Information, Table S1). However, breaking of the alkyne bond in phenylacetylene to form a styrene derivate is inevitably associated with a large activation barrier,[12] which explains why phenylacetylene does not form upright self-assemblies on gold by thermal activation at any temperature below the desorption threshold. A schematic in Figure 6c shows the relevant energies of the ground-state configurations relative to the flat-lying phenylacetylene molecules. Tip-induced hot electrons/holes injections overcome

high reaction energy barriers that prevent the reaction from occurring by thermal pathways.

The hot electron energy threshold for the assembly process was estimated to be +0.3−0.4 V by quantifying the size of the self-assembled structures as a function of scan rate (Figure 2a), comparable to the C≡C stretch modes of the gas-phase phenylacetylene molecule which have energy of 264 meV from both the database[25] and our DFT calculations. Therefore, the assembly reaction is most likely initiated by the vibrationally excited phenylacetylene in its ground electronic state, which is a common mechanism for STM-induced chemistry.[26,27] This mechanism is consistent with a comparatively low reaction yield for the assembly reaction and the fact that the lowest unoccupied molecular orbital (LUMO) of adsorbed phenylacetylene is centered at least 2.5 eV above the Fermi level,[20] precluding electron attachment at the tunneling bias of 0.4 V.

The disassembly at a distance proceeds through a more intriguing mechanism of delocalized excitation, which was recently reported for a number of molecules on metal surfaces.[28] In almost all cases, the reactions were induced by reactive electron attachment of hot electrons that propagate *via* the surface resonances of the metal surfaces.[28−30] The energy threshold for the hot-hole-induced reaction in our case is around −0.2 eV (Figure 6a), which necessitates that the highest occupied molecular orbital (HOMO) is in this energy range. Indeed, our theoretical calculations (Figure 6b and Supporting Information, Figure S5) revealed that not only is the HOMO of the styrene derivate strongly broadened, but its HOMO−LUMO gap is also very narrow when the styrene derivative is placed on a gold surface. The broadening and proximity of the HOMO to the Fermi level explains the low energy threshold.

## CONCLUSIONS

In conclusion, the electron-assisted direct control over the anchor bond chemistry has allowed us to self-assemble molecules on a surface that do not or even cannot self-assemble by thermal activation. The created saturation coverage of upright phenylacetylene molecules has a density of 3.1 molecules/nm$^2$, comparable to the dense $\sqrt{3}\times\sqrt{3}R30$ phase of alkanethiols/Au(111) (4.9 molecules/nm$^2$). Electron-induced self-assembly does not change the stoichiometry of the parent phenylacetylene molecule and does not significantly perturb the underlying metal surface while creating robust and strong chemical bonds at the metal−molecule interface. Moreover, the reaction is completely reversible, allowing us to manipulate the self-assembled layer from single molecule to mesoscopic scale. At present, the controlled assembly is limited to areas that are on the boundary of nanoscale and mesoscale dimensions. To become truly competitive with alkanethiols, electronic methodologies would need to scale correspondingly. We envision that, in the future, excitation with light, macroscopic electron beams, or a combination of the two can be invoked to gain local and global control over the self-assembly without thermal excitation, paving the way to new chemical design rules aimed at self-assembly of small and large molecules on demand and in a desired pattern for electronic, photonic, and energy applications.

## METHODS

**Sample and Tip Preparation.** Sample preparation and STM measurements were performed in an ultrahigh vacuum system (base pressure is better than $1 \times 10^{-10}$ mbar). Experiments were conducted with a home-built variable-temperature scanning tunneling microscopy, whose temperature can vary from 25 to 300 K. Phenylacetylene molecules were purified by the standard freeze−pump−thaw process. The Au(111) surface was cleaned by standard argon sputtering−annealing cycles before deposition of phenylacetylene molecules. The Au(111) substrate was kept at around 120 K during the molecular deposition. A commercial Pt−Ir tip was prepared by gentle field emission at a clean Au(111) sample. The bias voltage was applied on the sample during the STM observations. The STM images were analyzed using WsXM.[31]

**DFT Calculations.** Three sets of structures comprising a single molecule on Au were investigated with density functional theory (DFT). Each set contained several configurations. For phenylacetylene on Au, we investigated 12 configurations, which are characterized by the position of the center of the phenyl with respect to the Au atoms of the first, second, or third layer and by the rotation angle of the alkyne tail. They are very similar to the configurations investigated by Bilic *et al.*[32] for benzene on M(111), M = Cu, Ag, and Au, except that we have included 4 more configurations to account for different rotation angles of the alkyne tail. For both the styrene and the phenylvinylidene derivative on Au, we investigated 4 configurations. These are labeled as FCC, HCP, TOP, and bridge and are the same configurations studied by Ford *et al.*[12] Thus, in total, 20 configurations were modeled. Each was relaxed using the projector-augmented wave pseudopotentials (PAW)[33] with an energy cutoff of 400 eV, 3 × 3 × 1 K-point grid, dipole corrections, and with the exchange correlation potential approximated by the Perdew, Burke, and Ernzerhof approximation (PBE).[34] The molecule and the first layer of Au were allowed to relax until the atomic forces were smaller than 0.02 eV/Å.

All of the calculations were carried out with the software VASP.[35] For every configuration, the hexagonal unit cell has an in-plane lattice parameter *a* of 33.7 Å and *c*/*a* ratio of 0.93. The vacuum space, which is about 27 Å, is large enough to ensure that periodic images do not interact with each other. The Au substrate was represented with 4 layers.

The ordered structure in Figure 5c was obtained by using a hexagonal supercell with in-plane lattice parameter (*a*) of 11.88 Å and axial ratio (*c*/*a*) of 2.69. The vacuum space is kept as 13.5 Å from the top of the molecule to the bottom of the nearby image Au slab. The relaxation of this structure was carried out with VASP using the PAW pseudopotentials and PBE with an energy cutoff of 400 eV and a K-point mesh of 4 × 4 × 1. The molecules and the first layer of Au were allowed to relax until the atomic forces were smaller than 0.02 eV/Å.

The simulated STM images of the optimized structure shown in Figure 5d were obtained using Tersoff's formalism,[36] in which the current crucially depends on the local density of

states (LDOS) of the surface sampled. To obtain the constant current STM image, the LDOS surface with the same value is recorded in a top view manner. The changes with height in the LDOS surface above the Au(111) slab correspond to the tip retractions in the constant current mode STM measurement.

The LDOS of the optimized structure was calculated using the PWscf[37] software. Γ point sampling, the PBE pseudopotential, an energy cutoff of 544 eV, a Gaussian smearing of 0.02 eV, and +1 V sample bias were used.

*Conflict of Interest:* The authors declare no competing financial interest.

*Acknowledgment.* This research was conducted at the Center for Nanophase Materials Sciences (CNMS), which is sponsored at Oak Ridge National Laboratory by the Scientific User Facilities Division, Office of Basic Energy Sciences, U.S. Department of Energy. The work at NCSU was supported by DOE Grant DE-FG02-98ER45685. The computations were performed using the resources of the CNMS and the National Center for Computational Sciences at Oak Ridge National Laboratory. This research also used resources of the National Energy Research Scientific Computing Center, which is supported by the Office of Science of the U.S. Department of Energy under Contract No. DE-AC02-05CH11231.

*Supporting Information Available:* (1) Temperature dependence of the STM images of hexamers on Au(111) surface. (2) Series of STM images showing the island formation process. (3) The manipulation of the defects embedded in the self-assembled layer. (4) Relaxed structural models of phenylacetylene on Au(111) surface. (5) Calculated projected density of states of phenylacetylene on Au(111) surface. This material is available free of charge *via* the Internet at http://pubs.acs.org.

## REFERENCES AND NOTES

1. Fan, F. R. F.; Yang, J. P.; Cai, L. T.; Price, D. W.; Dirk, S. M.; Kosynkin, D. V.; Yao, Y. X.; Rawlett, A. M.; Tour, J. M.; Bard, A. J. Charge Transport through Self-Assembled Monolayers of Compounds of Interest in Molecular Electronics. *J. Am. Chem. Soc.* **2002**, *124*, 5550–5560.
2. Mantooth, B. A.; Weiss, P. S. Fabrication, Assembly, and Characterization of Molecular Electronic Components. *Proc. IEEE* **2003**, *91*, 1785–1802.
3. Ginger, D. S.; Zhang, H.; Mirkin, C. A. The Evolution of Dip-Pen Nanolithography. *Angew. Chem., In. Ed.* **2004**, *43*, 30–45.
4. Fenter, P.; Eberhardt, A.; Eisenberger, P. Self-Assembly of *N*-Alkyl Thiols as Disulfides on Au(111). *Science* **1994**, *266*, 1216–1218.
5. Love, J. C.; Estroff, L. A.; Kribel, J. K.; Nuzzo, R. G.; Whitesides, G. M. Self-Assembled Monolayers of Thiolates on Metals as a Form of Nanotechnology. *Chem. Rev.* **2005**, *105*, 1103–1169.
6. Vericat, C.; Vela, M. E.; Benitez, G.; Carro, P.; Salvarezza, R. C. Self-Assembled Monolayers of Thiols and Dithiols on Gold: New Challenges for a Well-Known System. *Chem. Soc. Rev.* **2010**, *39*, 1805–1834.
7. Poirier, G. E. Characterization of Organosulfur Molecular Monolayer on Au(111) Using Scanning Tunneling Microscopy. *Chem. Rev.* **1997**, *97*, 1117–1127.
8. Maksymovych, P.; Voznyy, O.; Dougherty, D. B.; Sorescu, D. C.; Yates, J. T. Gold Atom as a Key Structural Component in Self-Assembled Monolayers of Organosulfur Molecules on Au(111). *Prog. Surf. Sci.* **2010**, *85*, 206–240.
9. Schreiber, F. Structure and Growth of Self-Assembling Monolayers. *Prog. Surf. Sci.* **2000**, *65*, 151–256.
10. Alemani, M.; Peters, M. V.; Hecht, S.; Rieder, K. H.; Moresco, F.; Grill, L. Electric Field-Induced Isomerization of Azobenzene by STM. *J. Am. Chem. Soc.* **2006**, *128*, 14446–14447.
11. Comstock, M. J.; Levy, N.; Kirakosian, A.; Cho, J.; Lauterwasser, F.; Harvey, J. H.; Strubbe, D. A.; Frechet, J. M. J.; Trauner, D.; Louie, S. G.; *et al.* Reversible Photomechanical Switching of Individual Engineered Molecules at a Metallic Surface. *Phys. Rev. Lett.* **2007**, *99*, 038301–038305.
12. Ford, M. J.; Hoft, R. C.; McDonagh, A. M. Theoretical Study of Ethynylbenzene Adsorption on Au(111) and Implications for a New Class of Self-Assembled Monolayer. *J. Phys. Chem. B* **2005**, *109*, 20387–20392.
13. Walsh, M. A.; Walter, S. R.; Bevan, K. H.; Geiger, F. M.; Hersam, M. C. Phenylacetylene One-Dimensional Nanostructures on the Si(100)-2×1:H Surface. *J. Am. Chem. Soc.* **2010**, *132*, 3013–3019.
14. Sohn, Y.; Wei, W.; White, J. M. Phenylacetylene on Cu(111): Adsorption Geometry, Interfacial Electronic Structures and Thermal Chemistry. *J. Phys. Chem. C* **2007**, *111*, 5101–5110.
15. Iucci, G.; Carravetta, V.; Altamura, P.; Russo, M. V.; Paolucci, G.; Goldoni, A.; Polzonetti, G. XPS, NEXAFS and Theoretical Study of Phenylacetylene Adsorbed on Cu(100). *Chem. Phys.* **2004**, *302*, 43–52.
16. McDonagh, A. M.; Zareie, H. M.; Ford, M. J.; Barton, C. S.; Markovic, M. G.; Matisons, J. G. Ethynylbenzene Monolayers on Gold: A Metal-Molecule Binding Motif Derived from a Hydrocarbon. *J. Am. Chem. Soc.* **2007**, *129*, 3533–3538.
17. Rao, T. S. S.; Awasthi, S. Oxidative Cleavage of Carbon−Carbon Triple Bond—A Review. *J. Ind. Chem. Soc.* **2003**, *80*, 1129–1141.
18. Han, P.; Mantooth, B. A.; Skyes, E. C. H.; Donhauser, Z. J.; Weiss, P. S. Benzene on Au(111) at 4 K: Monolayer Growth and Tip-Induced Molecular Cascades. *J. Am. Chem. Soc.* **2004**, *126*, 10787–10793.
19. Jiang, N.; Zhang, Y. Y.; Liu, Q.; Cheng, Z. H.; Deng, Z. T.; Du, S. X.; Gao, H. J.; Beck, M. J.; Pantelides, S. T. Diffusivity Control in Molecule-on-Metal Systems Using Electric Fields. *Nano Lett.* **2010**, *10*, 1184–1188.
20. Li, Q.; Han, C. B.; Horton, S. R.; Cabrera, M. F.; Sumpter, B. G.; Lu, W. C.; Bernholc, J.; Maksymovych, P.; Pan, M. H. Supramolecular Self-Assembly of π-Conjugated Hydrocarbons *via* 2D Coorperative CH/π Interaction. *ACS Nano* **2012**, *6*, 566–572.
21. Yang, G. H.; Liu, G. Y. New Insights for Self-Assembled Monolayers of Organothiols on Au(111) Revealed by Scanning Tunneling Microscopy. *J. Phys. Chem. B* **2003**, *107*, 8746–8759.
22. Poirier, G. E.; Pylant, E. D. The Self-Assembly Mechanism of Alkanethiols on Au(111). *Science* **1996**, *272*, 1145–1148.
23. Pluchery, O.; Coustel, R.; Witkowski, N.; Borensztein, Y. Adsorption of Phenylacetylene on Si(100)-2×1: Kinetics and Structure of the Adlayer. *J. Phys. Chem. B* **2006**, *110*, 22635–22643.
24. Nishio, M. CH/π Hydrogen Bonds in Crystals. *CrystEngComm* **2004**, *6*, 130–158.
25. Phenylethyne. The NIST WebBook, http://webbook.nist.gov/.
26. Ho, W. Single-Molecule Chemistry. *J. Chem. Phys.* **2002**, *117*, 11033–11061.
27. Lauhon, L. J.; Ho, W. Single-Molecule Chemistry and Vibrational Spectroscopy: Pyridine and Benzene on Cu(001). *J. Phys. Chem. A* **2000**, *104*, 2463–2467.
28. MacLeod, J. M.; Duffin, J. L.; Fu, C. Y.; Rosei, F. Inducing Nonlocal Reactions with a Local Probe. *ACS Nano* **2009**, *3*, 3347–3351.
29. Maksymovych, P.; Dougherty, D. B.; Zhu, X. Y.; Yates, J. T. Nonlocal Dissociative Chemistry of Adsorbed Molecules Induced by Localized Electron Injection into Metal Surfaces. *Phys. Rev. Lett.* **2007**, *99*, 016101-1–016101-4.
30. Nouchi, R.; Masunari, K.; Ohta, T.; Kubozono, Y.; Iwasa, Y. Ring of $C_{60}$ Polymers Formed by Electron or Hole Injection from a Scanning Tunneling Microscope Tip. *Phys. Rev. Lett.* **2006**, *97*, 196101-1–196101-4.
31. Horcas, I.; Fernandez, R.; Gomez-Rodriguez, J. M.; Colchero, J.; Gomez-Herrero, J.; Baro, A. M. WSXM: A Software for Scanning Probe Microscopy and a Tool for Nanotechnology. *Rev. Sci. Instrum.* **2007**, *78*, 013705-1–013705-8.
32. Bilic, A.; Reimers, J. R.; Hush, N. S.; Hoft, R. C.; Ford, M. J. Adsorption of Benzene on Copper, Silver, and Gold Surfaces. *J. Chem. Theory Comput.* **2006**, *2*, 1093–1105.
33. Blochl, P. E. Projector Augmented-Wave Method. *Phys. Rev. B* **1994**, *50*, 17953–17979.

34. Perdew, J. P.; Burke, K.; Ernzerhof, M. Generalized Gradient Approximation Made Simple. *Phys. Rev. Lett.* **1996**, *77*, 3865–3868.
35. Kresse, G.; Hafner, J. *Ab Initio* Molecular Dynamics for Liquid Metals. *Phys. Rev. B* **1993**, *47*, 558–561.
36. Tersoff, J.; Harmann, D. R. Theory of The Scanning Tunneling Microscope. *Phys. Rev. B* **1985**, *31*, 805–813.
37. Giannozzi, P.; Baroni, S.; Bonini, N.; Calandra, M.; Car, R.; Cavazzoni, C.; Ceresoli, D.; Chiarotti, G. L.; Cococcioni, M.; Dabo, I.; *et al.* QUANTUM SSPRESSO: A Modular and Open-Source Software Project for Quantum Simulations of Materials. *J. Phys.: Condens. Mater.* **2009**, *21*, 395502-1–395502-19.